

## A numerical method for the dynamics of non-spherical cavitation bubbles

L. Guerri

Istituto di Matematica, Università di Pavia, 27100 Pavia, Italy

G. Lucca and A. Prosperetti

Istituto di Fisica, Via Celoria 16, 20133 Milano, Italy

Abstract

In this paper a boundary integral numerical method for the dynamics of non-spherical cavitation bubbles in inviscid incompressible liquids is described. A very efficient feature of this approach is that it involves only surface values of the velocity potential and its first derivatives, thus avoiding the problem of solving the Laplace equation in the entire domain occupied by the liquid. To illustrate the performance of the method the collapse of a bubble in the vicinity of a solid wall and the collapse of three bubbles with collinear centers are considered.

Introduction

The development of the study of the dynamics of non-spherical bubbles has been seriously hindered in the past by the lack of computational tools applicable to severe deformations of the spherical shape. Existing methods<sup>1-4</sup> are cumbersome to implement and require long execution times. These problems have prevented their widespread usage and common acceptance. In this study we shall present a much more efficient method based on the boundary integral approach<sup>5</sup> which can be implemented in a relatively small number of program instructions (500-600). It is flexible, precise, and requires short execution times (typically 3-5 minutes on a Univac 1100). The method is applicable to irrotational, incompressible, inviscid flow and we present an axisymmetric version of it. To illustrate the results obtainable in this way we consider the Rayleigh problem, one of the cases studied by Plesset and Chapman<sup>1</sup>, and the collapse of three bubbles with collinear centers.

Mathematical formulation

We consider the flow induced by one or more bubbles in a liquid occupying a domain  $\Omega$  bounded by the surface of the bubbles,  $S_b$ , rigid boundaries,  $S_r$ , and a "surface at infinity"  $S_\infty$ . In the hypotheses of inviscid irrotational flow the velocity field  $\underline{u}$  can be derived from a potential,  $\underline{u} = \nabla\phi$ , and the mathematical problem can be put in the form<sup>1</sup>

$$\nabla^2\phi = 0 \quad \text{in } \Omega, \quad (1)$$

$$\frac{\partial\phi}{\partial n} = 0 \quad \text{on } S_r, \quad (2)$$

$$\frac{d\phi}{dt} = \frac{1}{2}|\nabla\phi|^2 + \frac{P_\infty - P_b}{\rho} \quad \text{on } S_b, \quad (3)$$

$$\frac{d\underline{x}}{dt} = \nabla\phi \quad \text{on } S_b, \quad (4)$$

$$\phi \rightarrow 0, \quad p \rightarrow p_\infty \quad \text{on } S_\infty, \quad (5)$$

where  $p$  is the pressure,  $\rho$  is the density,  $\partial/\partial n$  is the normal derivative, and  $d/dt = \partial/\partial t + \nabla\phi \cdot$  is the convective derivative. The pressure in the bubble,  $P_b$ , and at infinity,  $P_\infty$ , are taken constant in this study, although this is by no means required by the method. Surface tension effects have been disregarded, but they can be included with relative ease.

The strategy of solution is in principle quite straightforward. Suppose that the position of the bubble surfaces  $S_b$  and the value of  $\phi$  on  $S_b$  are known at time  $t$ . Then Eq.(1) can be solved using the boundary conditions (2), (5), and the known  $\phi$  on  $S_b$ . From a knowledge of the potential it is then possible to evaluate the right-hand sides of (3) and (4), which allows

the computation of the new configuration of  $S_b$  and of the potential on it at time  $t+\Delta t$ . The cycle is then repeated.

The crucial step in this procedure is the solution of the potential problem. In the past this has been done by finite differences<sup>1,2,4</sup> or by singularity methods<sup>6,7</sup>. The first approach is wasteful because it requires that the potential be known over the entire domain  $\Omega$ , although only free surface values are needed. In addition, the position of  $S_b$  does not coincide with grid nodes in general, which leads to well-known problems of accuracy, coding, and others. The second method avoids the explicit solution of (1) because the assumed form for  $\phi$  already is a solution of the Laplace equation. However a certain amount of guessing is necessary, and it is not clear whether very extreme bubble deformations can be described satisfactorily with this approach. Our technique, based on the boundary integral, or boundary element, method<sup>5</sup>, retains the advantages of the singularity method while avoiding its disadvantages since it is based on an exact relation, Green's identity. This identity for a point  $\underline{x}$  belonging to  $S_b$  or  $S_r$  has the form<sup>5</sup>

$$\phi(\underline{x}) = \frac{1}{2\pi} \int_{S_b+S_r} \{ |\underline{x}-\underline{x}'|^{-1} \frac{\partial \phi}{\partial n'} - \phi(\underline{x}') \frac{\partial}{\partial n'} |\underline{x}-\underline{x}'|^{-1} \} ds' \quad (6)$$

In conditions of axial symmetry, which we assume, this relation can be simplified by carrying out the integration over the azimuthal angle explicitly with the result

$$\phi(\underline{x}) = \int_{\Gamma_b+\Gamma_r} \{ G(\underline{x};\underline{x}') \frac{\partial \phi(\underline{x}')}{\partial n'} - H(\underline{x};\underline{x}') \phi(\underline{x}') \} ds' \quad (7)$$

In this equation  $\underline{x}$  and  $\underline{x}'$  belong to a meridian (half)plane passing through the axis of symmetry and  $\Gamma_b$  and  $\Gamma_r$  are the traces on this plane of  $S_b$  and  $S_r$  respectively;  $s'$  is the arc length on these curves  $\Gamma$ . In the meridian plane we choose a Cartesian system of coordinates  $(r,z)$ , of which the  $z$ -axis coincides with the axis of symmetry. Then  $G,H$  have the form

$$G(r,z;r',z') = \frac{2r'}{\pi\sqrt{A}} K(m) \quad , \quad H(r,z;r',z') = \frac{2r'}{\pi} \frac{\partial}{\partial n'} \{ K(m) \sqrt{A} \} \quad , \quad (8)$$

where  $A = (r+r')^2 + (z-z')^2$ ,  $m=4rr'/A$ , and  $K$  denotes the complete elliptic integral of the first kind.

In the applications to be described in this paper the existence of the rigid boundary is accounted for by introducing a system of "image" bubbles. Therefore condition (2) will be implicitly satisfied and it is no longer necessary to indicate explicitly the rigid boundary  $S_r$  or  $\Gamma_r$ . Accordingly, we shall not carry these symbols along in the following equations and we shall denote  $\Gamma_b$  simply by  $\Gamma$ .

#### Numerical method

Since  $\phi$  is known on  $\Gamma$  from the previous time step, Eq.(7) can be regarded as an integral equation for  $\partial\phi/\partial n'$ . To solve it, we approximate the line  $\Gamma$  by a polygonal line consisting of  $n$  segments  $\Gamma_j$  on each of which  $\phi$  and  $\partial\phi/\partial n'$  are taken constants. (We have also made some numerical experiments assuming a linear variation of  $\phi$  obtaining virtually identical results). In this way we obtain from (7) a linear system

$$\sum_{j=1}^n a_{ij} w_j = b_i \quad , \quad i = 1, 2, \dots, n \quad (9)$$

where  $w_j = \partial\phi(\underline{y}_j)/\partial n'$  can be interpreted as the value of the normal velocity at the midpoint  $\underline{y}_j$  of  $\Gamma_j$  and

$$a_{ij} = \int_{\Gamma_j} G(r_1, z_1; r', z') ds' \quad , \quad b_i = \phi(\underline{y}_i) + \sum_{j=1}^n \int_{\Gamma_j} H(r_1, z_1; r', z') \phi(r', z') ds' \quad . \quad (10)$$

Here  $r_i, z_i$  are to be interpreted as the coordinates of the midpoint  $y_i$  of  $\Gamma_i$ . The integrals in (10) are performed numerically by a six-point Gaussian formula except for those over  $\Gamma_j = \Gamma_i$  for which the integrand has an (integrable) logarithmic singularity. A series expansion in the neighborhood of this singularity coupled with Simpson's formula over the rest of the interval is used in this case. The elliptic integrals are computed using the simple approximate formulae of Ref. 8. The tangential velocity along the bubble surface is computed to the same accuracy as the normal velocity as follows

$$v(y_i) = \frac{\phi(x_{i+1}) - \phi(x_i)}{|x_{i+1} - x_i|} \quad (11)$$

where  $x_{i+1}$  and  $x_i$  are the extrema of the segment  $\Gamma_i$ . The normal and tangential velocities computed in this way are then referred to the  $(r, z)$  system of coordinates and transported by linear interpolation from the midpoints to the extrema of the segments  $\Gamma_i$ .

At this point Eqs. (3) and (4) can be used to compute the advanced-time values of the positions of the vertices of the polygonal line and of the associated velocity potentials. For this purpose the following second-order formula is used

$$\phi_i(t_{n+1}) = (1-\tau^2) \phi_i(t_n) + \tau^2 \phi_i(t_{n-1}) + (1+\tau) \Delta t_n d\phi_i(t_n)/dt \quad (12)$$

where  $\tau = \Delta t / \Delta t_{n-1}$  and  $\Delta t = t_{n+1} - t_n$ . A similar relation is used to compute the new values  $r_i, z_i$  of the positions of  $x_i$ . The possibility of using higher order time integration formulae of this type is a distinctive advantage of the present method over finite-differences ones. This advantage stems from the fact that here it is possible to follow the individual trajectories of the vertices of the polygonal line during the entire calculation. The time step used in (12) is adjusted during the calculation so as to prevent excessive variations of  $\phi_i, r_i, z_i$  during a single step.

### Results

We shall present the results in terms of lengths and times made dimensionless with respect to  $R_0$ , the initial bubble radius, and  $t_0 = R_0 \{ \rho / (p_\infty - p_b) \}^{1/2}$ . The pressure inside the bubble and at infinity have been kept constant in all the examples discussed.

To test the reliability of the method and of the code we have first of all computed the collapse of a single spherical bubble in an unbounded liquid, the well-known Rayleigh problem. The calculation started to develop instabilities in the velocity for a bubble radius  $R = 1.411 \times 10^{-2}$ , radial velocity  $R = 483.7$ , at time  $t = 0.9162$ . It is well known that this spherical collapse is unstable. Therefore, the ability of the code to compute a decrease in radius by nearly two orders of magnitude with no smoothing techniques applied and within a maximum 1.8% deviation from sphericity is an indication of an excellent performance. The analytical result for the radial velocity for the value of the radius indicated above is  $R = 487.4$ , again in excellent agreement with the numerical result. Finally, the analytical value of the total collapse time is  $t_c = 0.91468$ , in very good agreement with the computed value, which practically corresponds to total collapse.

As a second test we have considered one of the cases studied by Plesset and Chapman<sup>1</sup>. Here the bubble collapses in the presence of a plane rigid wall, from which it is separated by a distance equal to half the initial radius at  $t=0$ . In the calculation the plane was simulated by introducing an image bubble equal and symmetrically located with respect to the real bubble. By taking advantage of the symmetry of the problem it is possible to maintain the number of unknowns in the system (9) equal to the number of segments of the real bubble. We show in Fig. 1 the bubble shapes at selected instants (heavy lines) and the trajectories of some of the points on the bubble surface (light lines). It is interesting to observe the very strong convergence of streamlines in the jet which evolves in the later stages of the collapse. The shapes of Fig. 1 agree with those of Ref. 1, but a more stringent comparison is afforded by the values of the velocity of the "north pole" of the bubble as computed by us (Fig. 2, upper line) and as given in Ref. 1 (Fig. 2, open circles). Although the comparison is good, some minor discrepancies exist the origin of which is not clear at the present time. It may be noted how-

ever from the shapes published by Plesset and Chapman<sup>1</sup> that some imprecision affects their method near the "north pole" of the bubble, where the tangent fails to be zero as it should. The lower line of Fig. 2 shows the time development of the velocity of the "south pole" of the bubble.

As a final example we consider the collapse of a system of three equal and equally spaced bubbles, with centers on the axis of symmetry. The evolution of the process is shown in Fig. 3 for initial bubble spacings of 0.5 (left), 0.2 (center), and 0.1 (right). Because of the symmetry of this situation only the upper bubble and the upper half of the middle bubble are shown in the figure. The collapse of the central bubble is strongly inhibited by that of the other two and its "poles" move very little. This effect of course increases with the proximity of the bubbles.

Finally, to give an idea of the computational requirements we present in Table 1 some information on the number of segments used (for all the examples this is the number of segments in the first quadrant of the  $(r,z)$  plane), the number of time steps, and the CPU needed for the calculation on a UNIVAC 1100/8. Note that we have not tried yet to optimize the method with respect to time step size and number of segments used. For instance, it is believed that the latter quantity, in the cases of Fig. 3, could be reduced substantially without appreciable loss of accuracy.

Table 1. Some details on the computation

Case	Number of segments	Number of time steps	CPU time(mins and secs)
Rayleigh problem	16	105	1 7
Figure 1	32	79	3 15
Figure 3, left	48	92	8 30
Figure 3, center	48	99	9 12
Figure 3, right	48	100	9 7

#### Conclusions

The boundary integral method described in the present study has proven to be a very efficient and accurate tool for the study of non-spherical bubble dynamics. It makes possible extensive investigations of non-spherical bubble behavior at a fraction of the effort and cost required by other methods. In addition to its value for specific problems, we think that this feature is particularly important in the present state of research in this field because in our opinion only numerical experiments can help develop the intuition necessary for further progress.

#### Acknowledgment

This study has been supported in part by Ministero della Pubblica Istruzione of Italy.

#### References

1. Plesset, M.S., and Chapman, R.B., "Collapse of an initially spherical vapour cavity in the neighborhood of a solid boundary," J. Fluid Mech., Vol. 47, pp. 283-290. 1971.
2. Chapman, R.B., and Plesset, M.S., "Nonlinear effects in the collapse of a nearly spherical cavity in a liquid," J. Basic Eng., Vol. 94, pp. 142-145. 1972.
3. Ivany, R.D., and Hammitt, F.G., "Cavitation bubble collapse in viscous compressible liquids-Numerical analysis," J. Basic Eng., Vol. 87, pp. 977-985. 1965.
4. Prosperetti, A., "On the dynamics of non-spherical bubbles," in Lauterborn, W. (Ed.) Cavitation and Inhomogeneities in Underwater Acoustics, Springer-Verlag 1980, pp. 13-22.
5. Jaswon, M.A., and Symm, G.I., Integral Equation Methods in Potential Theory and Elastostatics, Academic Press 1977.
6. Bevir, M.K., and Fielding, P.J., "Numerical solution of incompressible bubble collapse with jetting," in Ockendon, J.R., and Hodgkins, W.R. (Eds.) Moving Boundary Problems in Heat Flow and Diffusion, Clarendon Press 1975.
7. Blake, J.R., and Gibson, D.C., "Growth and collapse of a vapour cavity near a free surface," J. Fluid Mech., in press.
8. Hastings, C., Approximations for Digital Computers, Princeton University Press 1955.

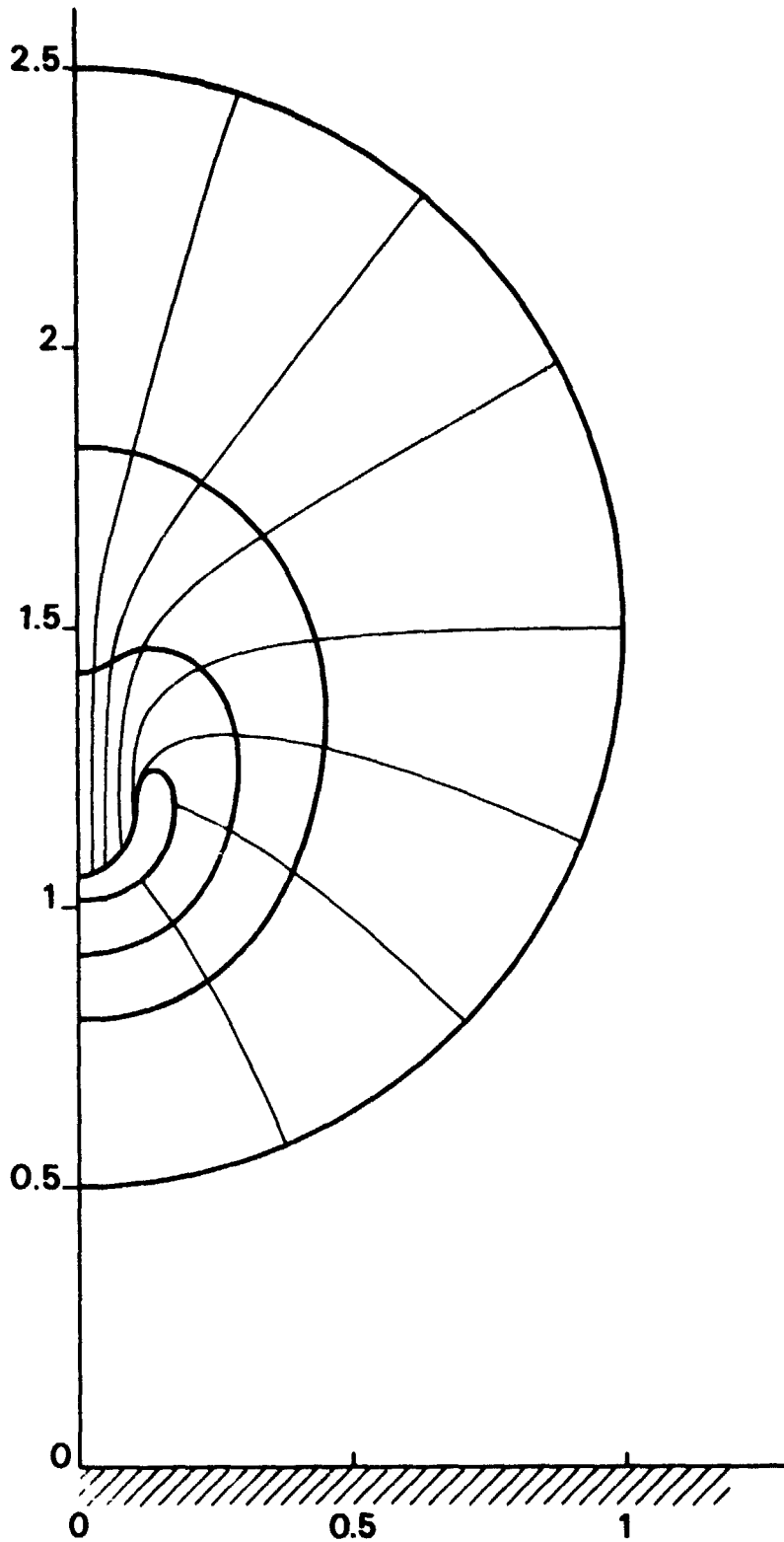


Figure 1. Collapse of an initially spherical bubble in the neighborhood of a solid plane from which it is separated by 0.5 times the initial radius. The shapes shown (heavy lines) are at  $t=0$ ,  $t=0.950$ ,  $t=1.010$ , and  $t=1.033$ . The collapse was completed during the time step after the last one shown. Light lines are particle trajectories.

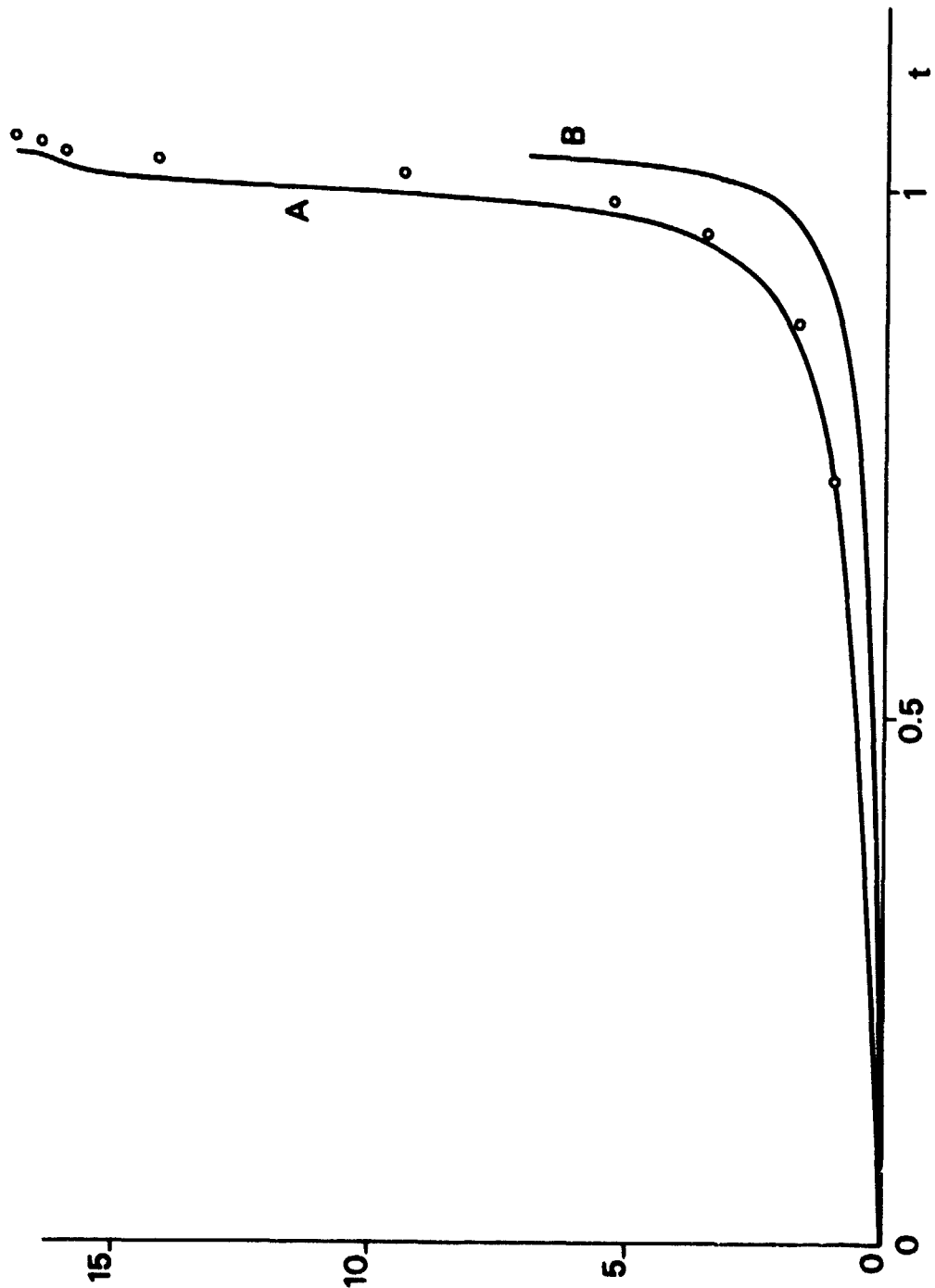


Figure 2. Comparison between the velocity of the "north pole" of the bubble of Fig. 1 (upper line) and the values given by Plesset and Chapman<sup>1</sup> (open circles). The lower line shows the velocity of the "south pole".

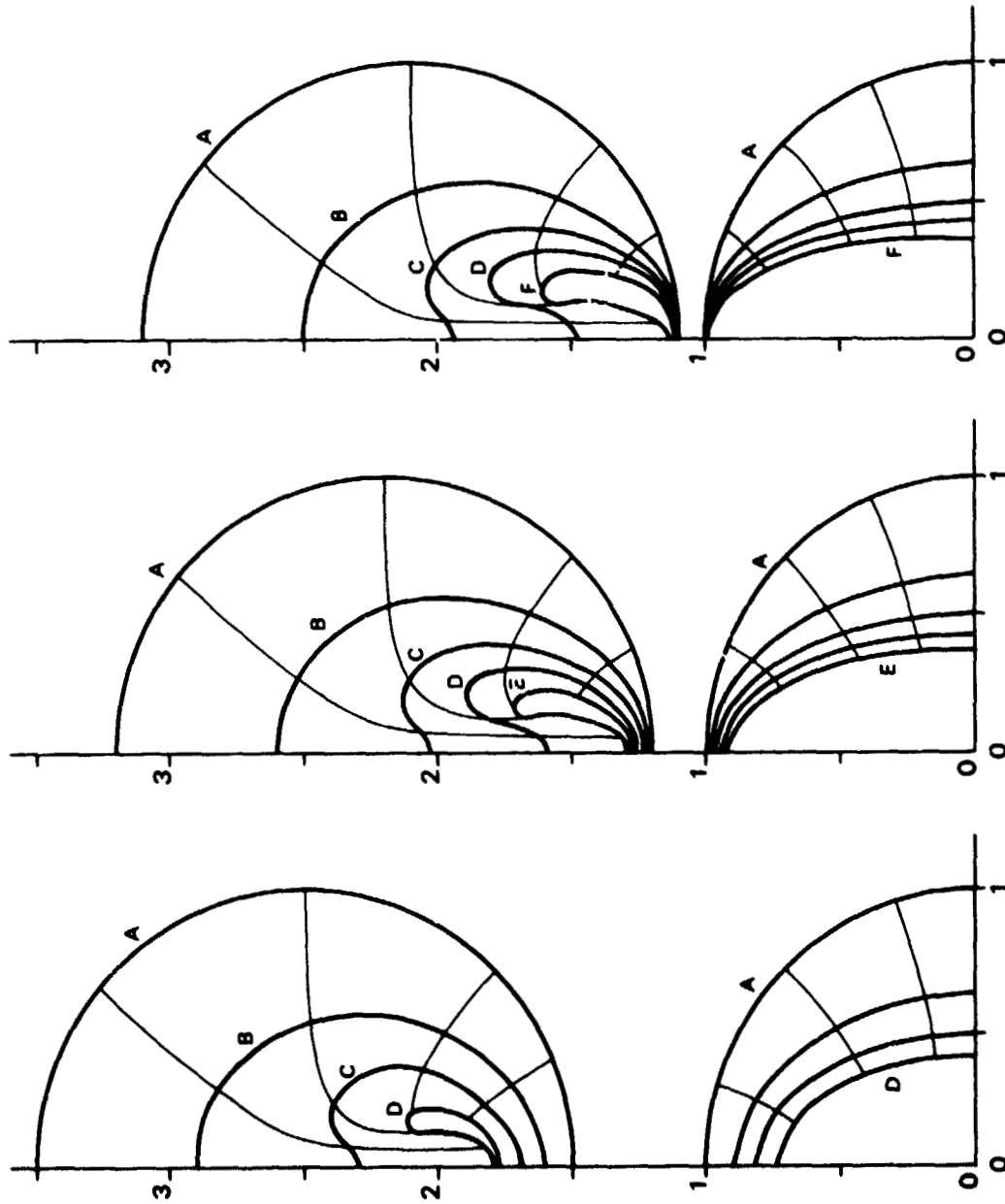


Figure 3. Collapse of three equal and equally spaced bubbles with collinear centers. The process is symmetric about the  $z=0$  plane. The initial bubble spacings are 0.5 (left), 0.2 (center), and 0.1 (right) times the initial radius. The shapes shown are for: A,  $t=0$ ; B,  $t=0.950$ ; C,  $t=1.063$ ; D,  $t=1.105$  (left and right),  $t=1.103$  (center); E,  $t=1.130$ ; F,  $t=1.135$ .